

Analysis of Her2/neu membrane protein clusters in different types of breast cancer cells using localization microscopy

R. KAUFMANN*[#], P. MÜLLER[†],[#], G. HILDENBRAND[†],
M. HAUSMANN[†] & C. CREMER*^{‡§}

*Applied Optics and Information Processing, Kirchhoff-Institute for Physics, University Heidelberg, Im Neuenheimer Feld, Heidelberg, Germany

[†]Peptide Chips and Nucleotide FISH, Kirchhoff-Institute for Physics, University Heidelberg, Im Neuenheimer Feld, Heidelberg, Germany

[‡]Institute for Pharmacy and Molecular Biotechnology, University Heidelberg, Im Neuenheimer Feld, Heidelberg, Germany

[§]Institute for Molecular Biophysics, The Jackson Laboratory, Bar Harbor, ME, U.S.A.

Key words. Her2/neu, mamma carcinoma, receptor clustering, statistical analysis, 3D dual colour localization microscopy.

Summary

The Her2/neu tyrosine kinase receptor is a member of the epidermal growth factor family. It plays an important role in tumour genesis of certain types of breast cancer and its overexpression correlates with distinct diagnostic and therapeutic decisions. Nevertheless, it is still under intense investigation to improve diagnostic outcome and therapy control. In this content, we applied spectral precision distance/position determination microscopy, a technique based on the general principles of localization microscopy in order to study tumour typical conformational changes of receptor clusters on cell membranes. We examined two different mamma carcinoma cell lines as well as cells of a breast biopsy of a healthy donor. The Her2/neu receptor sites were labelled by immunofluorescence using conventional fluorescent dyes (Alexa conjugated antibodies). The characterization of the Her2/neu distribution on plasma membrane sections of 176 different cells yielded a total amount of 20 637 clusters with a mean diameter of 67 nm. Statistical analysis on the single molecule level revealed differences in clustering of Her2/neu between all three different cell lines. We also showed that using spectral precision distance/position determination microscopy, a dual colour reconstruction of the 3D spatial arrangement of Her2/neu and Her3 is possible. This indicates that spectral precision distance/position determination microscopy could be used as

an enhanced tool offering additional information of Her2/neu receptor status.

Introduction

Human epidermal growth factor receptor 2 (Her2/neu) belongs to the family of the epidermal growth factor receptor (EGFR), which is composed of four related receptors (Her1 = EGFR = erbB1; Her2/neu = erbB2, Her3 = erbB3, Her4 = erbB4) (Yarden & Sliwkowski, 2001; Warren & Landgraf, 2006). The receptors are involved in signal transduction pathways that control and manage growth, division and differentiation processes of the cell.

The *Her2/neu* gene is located on the long arm of chromosome 17 (17q 12–21.32 / 35.1–35.14 Mb) and encodes a 185 kDa single-pass transmembrane protein receptor. These receptors consist of an extracellular ligand binding domain and a cytoplasmic tail with an intrinsic tyrosine kinase domain and multiple tyrosine phosphorylation sites (Schechter *et al.*, 1984; Coussens *et al.*, 1985; King *et al.*, 1985; Akiyama *et al.*, 1986; Stern *et al.*, 1986; Popescu *et al.*, 1989).

Previous research showed that overexpression of Her2/neu receptors exists in different cancers (Albanell & Baselga, 1999; Bacus *et al.*, 2002) and is associated with certain types of breast cancer. Amplification is the most common mechanism that correlates with Her2/neu receptor overexpression. This overexpression disturbs the normal control mechanisms (e.g. may lead to a temporally extended and enhanced intracellular signal transduction or activation and repression of numerous signal transduction pathways) of the cells and results in an aggressive tumour development.

In 20–30% of all breast cancers Her2/neu is overexpressed which correlates with a smaller probability of survival (Slamon

[#] RK and PM contributed equally to this work.

Correspondence to: R. Kaufmann, Applied Optics and Information Processing, Kirchhoff-Institute for Physics, University Heidelberg, Im Neuenheimer Feld 227 D-69120, Heidelberg, Germany. Tel: +49-6221-54-9274; fax: +49-6221-54-9112; e-mail: kaufmann@kip.uni-heidelberg.de

et al., 1987, 1989; Elledge & McGuire, 1992). Not only association of Her2/neu overexpressing tumours and poor prognosis, but also shorter overall survival and relapse rate of patient with Her2/neu overexpressing breast cancer relative to none overexpressing tumours are observed (Slamon *et al.*, 1987; 1989; Berchuck *et al.*, 1990).

The overexpressed Her2/neu receptor is a target for specific anticancer therapies of breast cancer. To improve prognostic and predictive information in diagnostic and therapy control, this makes further microscopy research on Her2/neu receptor interesting for clinical applications. Limitation of conventional far-field light microscopy, however, does not permit structural analysis below ~ 200 nm (Abbe, 1873; Rayleigh, 1896). Thus, to study Her2/neu receptor clusters in more detail, a technique may be required which provides a higher resolution and even single molecule information.

Because of the limited resolution of conventional light microscopy the distribution of Her2/neu has so far been investigated by electron microscopy (Yang *et al.*, 2007) and scanning near-field optical microscopy (Nagy *et al.*, 1999). Electron microscopy using immunogold labelling revealed a clustering of Her2/neu proteins with a mean cluster size of about nine proteins. Scanning near-field optical microscopy experiments also had shown clustering with a size in the range of 10^3 molecules and a diameter of about 500 nm. These various results show the need for a better characterization of the nanoscale expression pattern of the Her2/neu receptors.

Novel approaches in light microscopy, which overcome the restrictions of the Abbe limit, allow studying the distribution of membrane proteins. One of these methods is stimulated emission depletion microscopy, which was used for studies of the membrane protein syntaxin (Sieber *et al.*, 2007). High-resolved images indicated the formation of protein clusters with a diameter of 50 to 60 nm.

Another far-field sub-diffraction limit technique using visible light is localization microscopy, which additionally provides information of the position of each detected fluorophore. The fundamental concept of this method is to use fluorophores that can be switched between two different spectral states. Using this for temporal isolation of the single molecule signals, a spatial separation can be achieved. In this manner the positions of fluorophores can be determined even if they are close together (< 200 nm). Early approaches describe a localization precision of 50 nm and less for point like fluorescent objects (Burns *et al.*, 1985; Betzig, 1995; Bornfleth *et al.*, 1998; Cremer *et al.*, 1999; Esa *et al.*, 2001; Heilemann *et al.*, 2002). Using photo-activatable or photo-switchable fluorophores, various techniques like photoactivated localization microscopy (Betzig *et al.*, 2006), fluorescence activated localization microscopy (Hess *et al.*, 2006) and stochastic optical reconstruction microscopy (Rust *et al.*, 2006) allowed to visualize cellular structures with localization accuracies down to 20 nm. All these methods require special fluorophores, which can be

switched between two spectral states using an additional laser.

Recently, methods have been developed allowing the use of conventional fluorophores (e.g. fluorescent proteins and Alexa dyes) for localization microscopy (Fölling *et al.*, 2008; Heilemann *et al.*, 2008; Lemmer *et al.*, 2008). We applied for the presented study the method described in Lemmer *et al.*, 2008 [spectral precision distance/position determination microscopy (SPDM)], which uses the stochastic recovery of the fluorophores from a light-induced reversibly bleached state to the fluorescent state (Patterson & Lippincott-Schwartz, 2002; Sinnecker *et al.*, 2005; Hendrix *et al.*, 2008) for optical isolation of the single molecule signals. This allows a precise position determination of each detected fluorophore far below the conventional resolution limit. All acquired positions are merged to a localization image where the effective resolution is determined by the localization accuracy and the density of the detected signals. Baddeley *et al.* (2009) have recently shown that this method of localization microscopy enables the investigation of receptor distribution patterns in rat ventricular myocytes.

The work described here benefits from two crucial advantages of SPDM for analysis of the immunofluorescence labelled proteins. On the one hand high resolution enables the characterization of the Her2/neu distribution on the plasma membrane; on the other hand single molecule information provides the possibility for statistical analysis of the distribution of proteins. Algorithms based on the determination of distances between the detected single molecules indicated a formation of Her2/neu clusters and yielded a precise differentiation between the three cell lines (Cal-51: mamma carcinoma cell line with normal karyotype and SKBr3: mamma carcinoma cell line with *Her2/neu* amplification; AG11132: cells of a mamma biopsy of a healthy donor with normal karyotype). Our analyses utilizing local densities of the proteins allowed the determination of a cluster size of about 67 nm and the distribution of these protein clusters. Differences in the density within a Her2/neu cluster detected in the statistical analyses allow a determination and discrimination of the Her2/neu receptor status of cancer cell lines and may be a future tool to improve clinical diagnostics and therefore better prognosis.

By combining SPDM with SMI (spatially modulated illumination) microscopy we achieved a 3D dual colour reconstruction of the spatial arrangement of Her2/neu and Her3. The positions in all three directions of the protein clusters could be determined with an accuracy of about 25 nm.

Materials and methods

SPDM setup

Localization measurements were performed with a SPDM setup (Lemmer *et al.*, 2008). Optical isolation of signals

is achieved utilizing a light-induced reversibly bleached state (Patterson & Lippincott-Schwartz, 2002; Sinnecker *et al.*, 2005; Hendrix *et al.*, 2008) of the fluorophores. By illuminating the sample with a laser excitation intensity of 10 kW cm^{-2} to several 100 kW cm^{-2} some fluorophores are bleached irreversibly ($M_{fl} \rightarrow M_{ibl}$), but another amount is transferred to a reversibly bleached state ($M_{fl} \rightarrow M_{rbl}$). Stochastic recovery of these molecules to the fluorescent state ($M_{fl} \leftarrow M_{rbl}$) can be used for optical isolation of the detected single molecule signals. This method allows the usage of conventional fluorophores for localization microscopy.

For the present experiments a diode-pumped solid-state (DPSS) laser with a wavelength of 488 nm (Sapphire HP 488, Coherent, Dieburg, Germany) was used. A second DPSS laser (Sapphire 568, Coherent) is provided in the setup for excitation with 568 nm. The laser beam is expanded by a factor of 2.5 before being focused into the back focal plane of an oil immersion objective lens (HCX PL APO, $63\times$, NA = 0.7–1.4, Leica, Wetzlar, Germany). Fluorescent light emitted by the fluorophores in the sample passes a dichroic mirror (AHF Analysentechnik, Tübingen, Germany) and a blocking filter (F73–491, AHF Analysentechnik) before being focused onto the charge-coupled device chip of a very sensitive camera (SensiCam QE, PCO Imaging, Kehlheim, Germany). An additional lens can be mounted in the excitation pathway for increasing the laser intensity in the object plane to obtain appropriate conditions for the reversible photo bleaching.

Data acquisition and evaluation

For the present measurements data stacks consisting of several thousand images were recorded with an integration time of the camera of 50 to 150 ms. After conversion of the count numbers into photon numbers a differential image stack is calculated by subtracting the succeeding from the preceding frame. This has to be done to filter out the signals of the single molecules due to background noise and bleaching gradients of biological samples. After segmentation of the raw data, a 2D Gaussian is fitted to the single molecule signals to determine the positions of the detected molecules (Lemmer *et al.*, 2008, 2009; Gunkel *et al.*, 2009; Kaufmann *et al.*, 2009). Using this information a localization image is rendered by blurring the position of each detected molecule with a Gaussian corresponding to the individual localization accuracy. The effective optical resolution of this image is given by the density of detected signals and the localization accuracy. For the presented measurements the mean estimated localization accuracy was about 25 nm, the density of detected signals within the protein clusters about $2400 \mu\text{m}^{-2}$.

Cell culture, specimen preparation and immunofluorescence labelling

Cal-51 (German Resource Centre for Biological Material – DSMZ, Braunschweig, Germany) and SKBr3 (American Type

Culture Collection – ATCC, Manassas, VA, U.S.A.) are two mamma carcinoma cell lines from pleural effusion.

The first displays a normal diploid karyotype and an increased Her2/neu expression level. By contrast SKBr3 is a highly rearranged, hyper triploid cell line which shows translocations in nearly all chromosomes, except chromosomes 11 and 18. It carries an amplification of Her2/neu and thus overexpresses the Her2/neu receptor on the plasma membrane.

Cal-51 were cultivated in Dulbecco's Modified Eagle Medium (DMEM) supplemented with 20% Fetal Calf Serum (FCS), 1% l-glutamine, 1% penicillin/streptomycin and SKBr3 in McCoy's 5a medium with 10% FCS, 1% l-glutamine, 1% penicillin/streptomycin in a standard CO₂-incubator.

AG11132 are human mammary epithelial cells of a healthy donor (Coriell Institute, Camden, NJ, U.S.A.) and were established from normal tissue obtained at reduction mammoplasty. Cells were grown in mammary epithelial growth medium supplemented with $4 \mu\text{l ml}^{-1}$ bovine pituitary extract, $5 \mu\text{g ml}^{-1}$ insulin, 5 ng ml^{-1} epidermal growth factor, $0.5 \mu\text{g ml}^{-1}$ hydrocortisone (mammary epithelial growth medium BulletKit from Lonza, Walkersville, MD, U.S.A.), 10^{-5} M isoproterenol (Sigma-Aldrich, Hamburg, Germany), $5 \mu\text{g ml}^{-1}$ transferrin (Sigma-Aldrich) and 10 mM HEPES buffer (Sigma-Aldrich) in a standard CO₂-incubator.

All cells were seeded onto cover slips ($24 \times 24 \text{ mm}$, #1.5, Menzel-Gläser, Braunschweig, Germany) and allowed to attach and grown over night. Cells were fixed with 4% formaldehyde in Phosphate-Buffered Saline (PBS) when they reached 80% of confluency. After fixation immunofluorescence labelling (antibody dilution chosen for all experiments were 1:100) was carried out according to the manufacturers' protocols and subsequently embedded with ProLong® Gold antifade reagent (Invitrogen, Carlsbad, CA, U.S.A.). For further details an antibodies used for the present study see Table 1.

Results

Cluster analysis

For characterization of the protein clusters appropriate conditions were defined for a quantification of image parameters regarding a cluster. An algorithm based on local densities as well as on neighbouring conditions of each detected molecule was used.

In a first step the distance to the next neighbour for each detected molecule is determined. Afterwards all points are jittered randomly about the original positions with respect to their individual localization accuracy. These new positions are used again for determination of distances to the next neighbouring molecule. The whole procedure is repeated 100 times for the measurements presented here to render an image,

Table 1. Antibodies. Primary antibodies with their binding domains as well as the secondary antibodies with their associated fluorophores used in our experiments.

Abbreviation for binding domains and fluorophores	Primary antibodies	Host/isotype	Company
EXR = extracellular domain	Monoclonal anti-Her2/neu	Mouse IgG	Sigma-Aldrich
IntraTR = intracellular kinase domain	Polyclonal anti-Her2/neu	Rabbit IgG	Merck, Darmstadt, Germany
Secondary antibodies			
Alexa488	Alexa Fluor® 488	Goat anti-mouse IgG	Invitrogen
Alexa568	Alexa Fluor® 568	Goat anti-mouse IgG	Invitrogen
Alexa488	Alexa Fluor® 488	Goat anti-rabbit IgG	Invitrogen

which represents local densities as well as the localization accuracy of each detected molecule. A second image, also illustrating local densities, is calculated in such a way that every point in the resulting image is given an intensity expressing the sum of points located in a predefined area round each molecule position. For cluster determination both methods are combined to minimize artefacts of a particular one.

The critical density for a cluster was set to 530 points per μm^2 , which is equivalent to a minimum number of five neighbours around each detected molecule within a radius of 60 nm – the parameters for the neighbouring conditions. For the analysis of Her2/neu clusters only points are regarded belonging to areas where the local density is higher than the critical density. Parameters defining this threshold were chosen according to the following approach: a random distribution of points with the same mean density as the localization image was generated. In such a distribution clusters are formed by chance. To eliminate these in the localization data, the parameters for the critical density were set to a value, for which the probability of having clusters by chance in a random distribution drops to about 0.1%.

The second step of the algorithm includes a morphological closing to transform the clusters consisting of individual points into coherent objects. After data segmentation all characteristic quantities can be computed. Figure 1 illustrates by an example how protein clusters are found using this algorithm. Figure 1(C) shows the morphological closed pattern (labelled in orange) of several Her2/neu clusters with different sizes on the plasma membrane.

We determined a mean diameter of 67 nm with a standard deviation of 21 nm for the 20 637 Her2/neu clusters located on membrane sections of 176 different cells in total (see Fig. 2). Included in these measurements are the two cancerous cell lines (Cal-51 and SKBr3) with various antibody labelling (extracellular domain [EXR]-Alexa488, EXR-Alexa568 and intraTR-Alexa488) and the AG11132 cells labelled with EXR-Alexa488 (see 'Materials and methods'). The mean density of detected signals per cluster was 2434 points per μm^2 with a standard deviation of 852 points per μm^2 . A

significant difference for labelling or cell type concerning the size of clusters could not be observed.

Single molecule analysis

Investigations on the distribution of single molecules were done by determination of the distances between the detected fluorophores. Data for these distance analyses were provided by 94 SPDM measurements of Her2/neu on the three different cell lines labelled with EXR-Alexa488. For each localization measurement an image with randomly distributed points of the same mean density and total amount of points was simulated for comparison. Both, the distances to the next neighbouring molecule (data not shown) and distances from each molecule to all the others were investigated for the localization data containing all detected molecules as well as for filtered data containing only the positions of those molecules which are located in a cluster. All measurements revealed non-randomly distributed proteins on the plasma membrane. We observed an increasing number of short distances in the measurements as compared to a random distribution with the same density of points. This clearly indicates clustering of Her2/neu. Moreover, differences between the three cell lines could be noticed, even between the two cancerous cell lines. The histograms in Fig. 3(B) and (C) show that the distribution of distances in SKBr3 cells had a significantly higher maximum at short distances compared to Cal-51. The cells of the line AG11132 feature only a small amount of short distances compared to a random distribution.

Furthermore, the number of detected signals per cluster versus cluster diameter has been investigated for the different cell lines. Again, the cells of a healthy donor showed a different distribution compared to the cancerous cells. Figure 3(A) illustrates that for a certain cluster diameter the number of detected signals per cluster is lower in cells of a healthy donor.

Both analyses on the single molecule level revealed a Her2/neu protein density within the clusters that is dependent on the chosen type of cell line. In AG11132 cells notably fewer proteins are located within a cluster compared to Cal-51 and SKBr3 cells. Regarding the results of the distance analysis

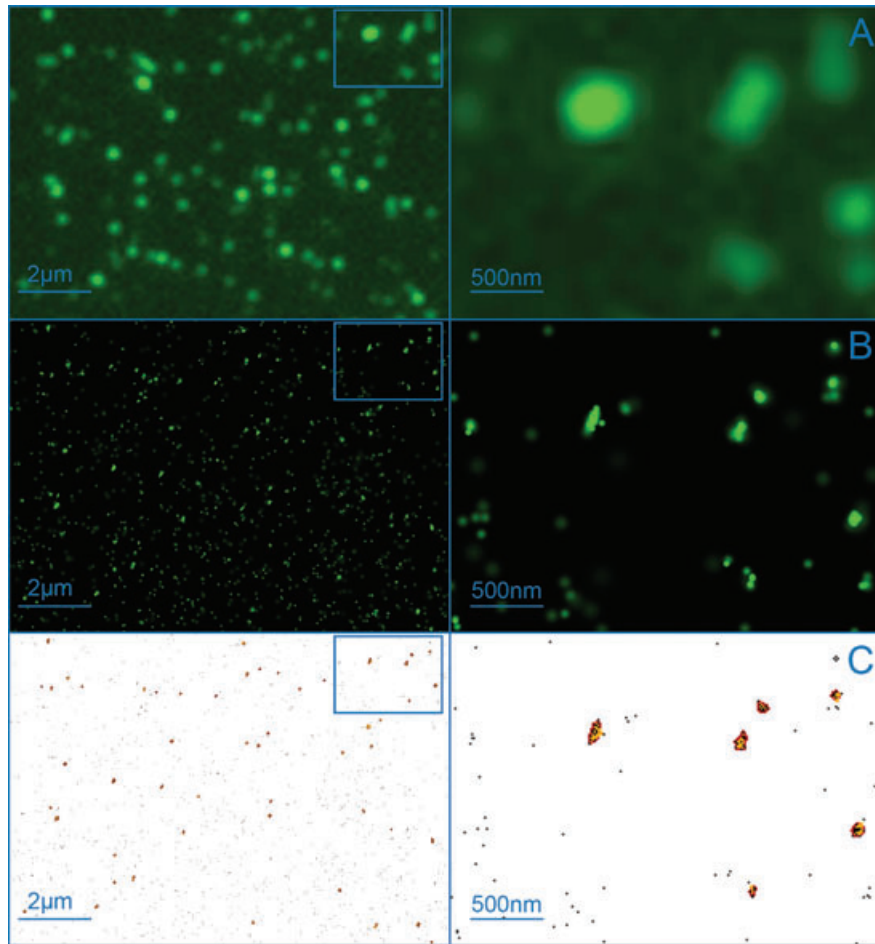


Fig. 1. Her2/neu clusters on membrane of a SKBr3 cell. (A): conventional wide-field fluorescence image of Her2/neu proteins on the plasma membrane of a SKBr3 cell. Her2/neu was labelled with Alexa488 and excited by a laser with a wavelength of 488 nm, respectively. (B): localization image of the same section. Intensity indicates the local density of detected fluorophores. Individual localization accuracy is rendered by a Gaussian blur. (C): results of the cluster finding algorithm. Positions of single molecules are marked as black dots. Clusters found by the algorithm are labelled in orange. Parameters were set to a critical local density of 530 points per μm^2 .

shown in Fig. 3(B) and (C) it was even possible to distinguish between the two cancerous cell lines. The density of Her2/neu within a cluster is slightly but significantly higher in the SKBr3 cells than in Cal-51 cells.

3D reconstruction of dual colour measurements of Her2/neu and Her3

So far all measurements and analyses presented in this study were performed on 2D data. In a first approach we could show that it is also possible to investigate the protein distribution of Her2/neu and Her3 in 3D. Therefore we used the combination of SPDM and SMI microscopy (Albrecht *et al.*, 2002; Hildenbrand *et al.*, 2005; Reymann *et al.*, 2008) according to Lemmer *et al.* (2008) and extended the setup for dual colour SPDM measurements. A standing wave field of the laser in the object space is generated via two opposing

objectives. An object scan and a phase scan of the region of interest yields the possibility of gathering the relative axial positions and extensions of the protein clusters. This information can be combined with the lateral positions of the detected single molecules in an SPDM measurement performed afterwards.

For the 3D reconstruction AG11132 cells were used with Alexa488 labelled Her2/neu receptors and Alexa568 labelled Her3 receptors. SMI and SPDM measurements were done sequentially for both dyes using lasers with a wavelength of 568 and 488 nm, respectively. For the correction of chromatic shifts in the lateral directions as well as in the axial direction we used fluorescent microspheres (TetraSpeck, Invitrogen) with a diameter of 100 nm placed on the membrane of the cells and on the surface of the cover slip. In Fig. 4(D) and (E), a 3D reconstruction of a dual colour SPDM measurement is shown. The positions of the clusters in each direction could

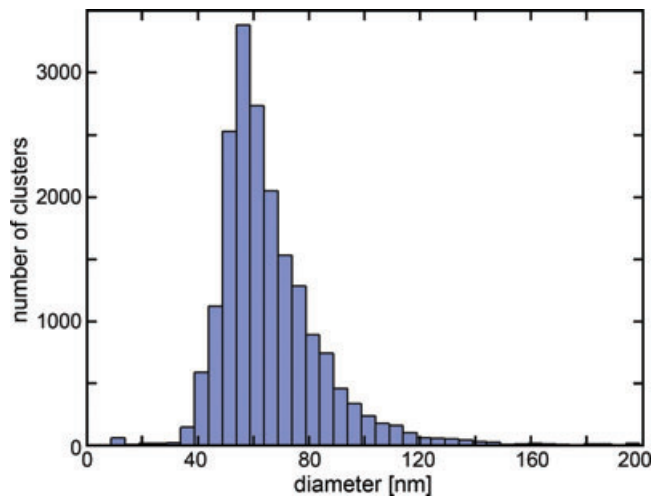


Fig. 2. Histogram of Her2/neu cluster size. The distribution of the diameter has a mean value of 67 nm and a standard deviation of 21 nm. For the determination 20 637 Her2/neu proteins of 176 SPDM measurements were analysed. All three cell lines are included.

be determined with a mean accuracy of about 25 nm. This allows a 3D investigation of the distribution of Her2/neu and Her3 on the membrane of a cell. In comparison to the 2D SPDM image some signals are missing in the 3D rendering. This is partly due to poor information of phase or object scan of some protein clusters. Objects without clearly determinable positions or extension in axial direction are lacking in the 3D rendering process. Due to a higher sensitivity for detection of single molecules in the localization image, signals not detected in the wide-field scan are also missing in the 3D rendering.

Discussion

General introduction

In recent years, sub-diffraction limit light microscopy methods have grown into sophisticated imaging techniques in biomedical sciences. Particularly localization microscopy, offering both single molecule information and an effective optical resolution down to the 20 nm regime, reveals more and more biological and medical applications.

Realizations of experiments

In this report, we used conventional wide-field fluorescence microscopy as well as SPDM, a localization microscopy technique. The high-resolution immunofluorescence images allow the characterization of Her2/neu clusters and their distribution on the plasma membrane. These results are comparable to previous studies performed with different microscopy techniques.

Algorithms based on the determination of local densities and distance analyses between the single detected molecules

revealed a novel insight into Her2/neu distribution pattern on the plasma membrane of cells of a healthy donor and two different cancerous cell lines.

Her2/neu distribution pattern

The algorithms developed for analysis and determination of protein clusters (in this case the Her2/neu receptors) revealed a mean cluster size of 67 nm. The evaluation of 20 637 protein clusters of membrane sections of 176 different cells showed that cluster size is independent concerning these three biologically different cell lines as well as the labelling methods in regard to their antibody epitope binding behaviour. This is in accordance with the observations presented in a publication of Nagy *et al.* (1999). They illustrated that cluster sizes are independent of the total number of Her2/neu proteins expressed per cell and the number of molecules in a single cluster.

Statistical analyses on the single molecule level

Further results of our presented work highlighted a statistical distance analysis on the single molecule level, which can be used as an additional factor for the discrimination of different cell types in regard to their karyotypes and Her2/neu expression on the plasma membrane. We used two mamma carcinoma cell lines from pleural effusion. Cal-51 displays a normal karyotype concerning copy numbers of *Her2/neu* genes. SKBr3 carries a copy number amplification of *Her2/neu* and thus overexpresses the Her2/neu receptor on the plasma membrane. AG11132 (healthy human mammary epithelial cells) were chosen to compare the two cancer cell lines with a healthy one of the same origin.

Our distance analysis yielded a distinct accumulation of small distances compared to randomly distributed points with the same density for all three cell types (see Fig. 3B). This is an additional indication for general clustering of Her2/neu. Besides that, this analysis allowed a distinct differentiation of the three cell lines according to the distributions of distances between the detected molecules. In AG11132 cells the amount of distances below 100 nm was many times lower than in the cancerous cell lines. A comparison of the number of detected signals per cluster versus cluster diameter revealed a higher density of proteins within a cluster in the cancerous cells lines than in the healthy one. This is consistent with the previous result, which had shown that the cluster diameter is independent of the cell line. Both results indicate that the difference between the cell lines is mainly expressed as the density of Her2/neu proteins within a cluster. Here, not only differences between the healthy and the cancerous cells were determined, it was even possible to distinguish between Cal-51 and SKBr3 cells. The increasing number of *Her2/neu* copies usually correlates with Her2/neu overexpression and is strongly compatible with an

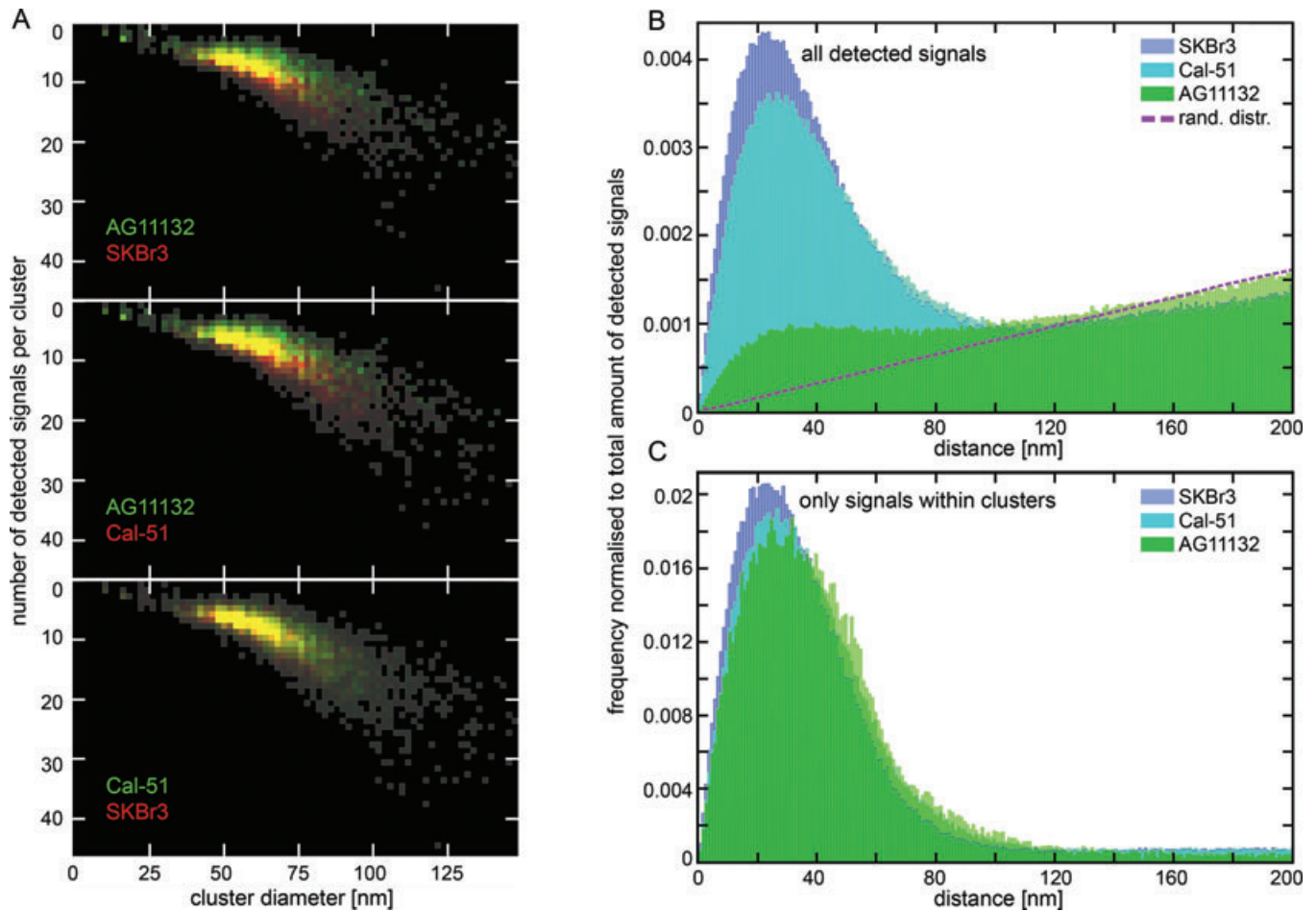


Fig. 3. Comparison of the three different cell lines on the single molecule level. (A): 2D histograms show the number of detected signals per cluster versus cluster diameter. The different cell types are colour coded; frequency is coded as brightness of the bins. Differences between the cells of a healthy donor (AG11132) and the cancerous cell lines are recognisable, whereas the distributions for Cal-51 and SKBr3 are very similar. (B): all distances up to 200 nm between the individual molecules occurring in the localization measurements are shown. (C): same analysis done only for the signals within the clusters. In both histograms the frequency of finding a particular distance is normalized to the total amount of determined distances respectively for both cases. Differences between all the different cell lines are clearly visible.

increase of smaller distances between the detected Her2/neu proteins.

The pathological testing of Cal-51, SKBr3 and AG11132 with Herceptin® on the single cell level will be subject of further investigation and will help to categorize our research more clearly in comparison to medical diagnostics.

Because the method described here is based on the application of single cells, tumour cells circulating in the blood of mamma carcinoma patients (Pachmann *et al.*, 2001, 2005b; Ring *et al.*, 2004) could be used for further analysis. These circulating tumour cells can be detected in many stages of the disease and after treatment. They respond to systemic therapy comparable to mamma tumours (Pachmann *et al.*, 2005a).

The variability of Her2/neu receptor expression is considered to be an important factor in breast cancer

prognosis. A more precise characterization of the Her2/neu protein distribution presented in this work will lead to a better understanding of the biological behaviour of membrane proteins which are involved in carcinogenesis.

Spatial arrangements of Her proteins in 3D

For a first insight on the spatial arrangement of Her proteins we performed a 3D dual colour SPDM measurement. Therefore Her2/neu was labelled with Alexa568 conjugated antibody, whereas Her3 was labelled with Alexa488 conjugated antibody. We could show that it is possible to determine the positions and extensions of the protein clusters in all three directions with accuracies in the 25 nm range. In the near future multicolour and 3D localization microscopy combined with quantitative analysis will help to understand the spatial

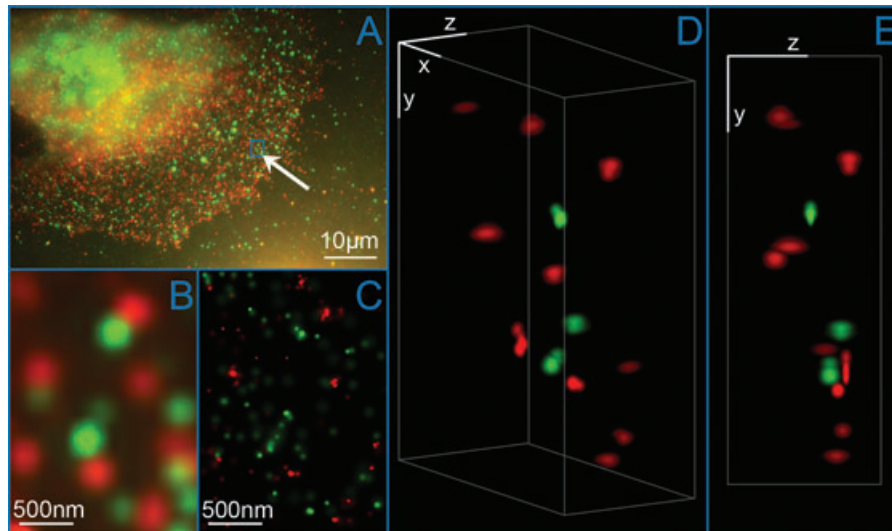


Fig. 4. 3D reconstruction of dual colour acquisition of Her2/neu and Her3. (A): conventional wide-field fluorescence image of an AG11132 cell. Her3 is labelled with Alexa488 (green) and Her2/neu with Alexa568 (red). (B): magnified image of a small area of (A) (marked by arrow). (C): localization microscopy image of the same region of interest as in (B). (D) and (E) show a 3D reconstruction of the protein clusters using the combination of SPDM and SMI microscopy. Scale bars in (D) and (E) are 500 nm in each direction.

arrangements of proteins in morphological intact cells more clearly.

Summary

To summarize, the study presented here shows that SPDM a sub-diffraction limit light microscopy technique can be applied for the characterization of the pattern of membrane proteins like Her2/neu and for differentiation between healthy and cancerous cell lines as well as between different types of cancerous ones.

This discrimination parameter of the protein distribution pattern enables, besides the Herceptin[®] test and fluorescence *in situ* hybridization, a supporting way to characterize and determine the Her2/neu status of cancer patients more precisely. Due to the correlation of the Her2/neu status with a bad prognosis and chance of survival this technique might improve the adaptation of therapy for cancer patients.

Acknowledgements

The financial supports of the University Heidelberg (Frontier Project grant to M. Wassenegger); of the Deutsche Forschungsgemeinschaft (SPP1128) and of the European Union (*In Vivo* Molecular Imaging Consortium, www.molimg.gr) to Christoph Cremer and of the Federal Ministry of Education and Research (BMBF) (Services@MediGRID) to Michael Hausmann are gratefully acknowledged. We also thank our colleagues Paul Lemmer, Manuel Gunkel, Thomas Ruckelshausen, Yanina Weiland, Heinz Eipel, Jutta Schwarz-Finsterle, Götz Pilarczyk and Margund Bach for great support.

References

- Abbe, E. (1873) Beiträge zur Theorie des Mikroskops und der mikroskopischen Wahrnehmung (Contributions to the theory of the microscope and microscopic observation). *Archiv f. mikroskopische Anatomie* **9**, 411–468.
- Akiyama, T., Sudo, C., Ogawara, H., Toyoshima, K. & Yamamoto, T. (1986) The product of the human *c-erbB2* gene: a 185-kilodalton glycoprotein with tyrosine kinase activity. *Science* **232**, 1644–1646.
- Albanell, J. & Baselga, J. (1999) The ErbB receptors as targets for breast cancer therapy. *J. Mammary Gland Biol. Neoplasia* **4**, 337–351.
- Albrecht, B., Failla, A.V., Schweitzer, A. & Cremer, C. (2002) Spatially modulated illumination microscopy allows axial distance resolution in the nanometer range. *Appl. Opt.* **41**, 80–87.
- Bacus, S.S., Altomare, D.A., Lyass, L. *et al.* (2002) AKT2 is frequently upregulated in HER-2/neu-positive breast cancers and may contribute to tumor aggressiveness by enhancing cell survival. *Oncogene* **21**, 3532–3540.
- Baddeley, D., Jayasinghe, I.D., Lam, L., Rossberger, S., Cannell, M.B. & Soeller, C. (2009) Optical single-channel resolution imaging of the ryanodine receptor distribution in rat cardiac myocytes. *Proc. Natl. Acad. Sci. U S A* **106**, 22275–22280.
- Berchuck, A., Kamel, A., Whitaker, R. *et al.* (1990) Overexpression of HER-2/neu is associated with poor survival in advanced epithelial ovarian cancer. *Cancer Res.* **50**, 4087–4091.
- Betzig, E. (1995) Proposed method for molecular optical imaging. *Opt. Lett.* **20**, 237–239.
- Betzig, E., Patterson, G.H., Sougrat, R. *et al.* (2006) Imaging intracellular fluorescent proteins at nanometer resolution. *Science* **313**, 1642–1645.
- Bornfleth, H., Sätzler, K., Eils, R. & Cremer, C. (1998) High-precision distance measurements and volume-conserving segmentation of objects near and below the resolution limit in three-dimensional confocal fluorescence microscopy. *J. Microsc.* **189**, 118–136.

- Burns, D.H., Callis, J.B., Christian, G.D. & Davidson, E.R. (1985) Strategies for attaining superresolution using spectroscopic data as constraints. *Appl. Opt.* **24**, 154–161.
- Coussens L., Yang-Feng T.L., Liao Y.C. *et al.* (1985) Tyrosine kinase receptor with extensive homology to EGF receptor shares chromosomal location with neu oncogene. *Science* **230**, 1132–1139.
- Cremer, C., Edelmann, P., Bornfleth, H., Kreth, G., Muench, H., Luz, H. & Hausmann, M. (1999) Principles of spectral precision distance confocal microscopy of molecular nuclear structure. *Handb. Comp. Vis. Appl.* **3**, 839–857.
- Elledge, R.M. & McGuire, W.L. (1992) Prognostic factors in axillary node-negative breast cancer. *Cancer Treat. Res.* **61**, 3–19.
- Esa, A., Edelmann, P., Trakthenbrot, L., Amariglio, N., Rechavi, G., Hausmann, M. & Cremer, C. (2001) Three-dimensional spectral precision distance microscopy of chromatin nanostructures after triple-colour DNA labelling: a study of the BCR region on chromosome 22 and the Philadelphia chromosome. *J. Microsc.* **199**, 96–105.
- Fölling, J., Bossi, M., Bock, H. *et al.* (2008) Fluorescence nanoscopy by ground-state depletion and single-molecule return. *Nat. Methods* **5**, 943–945.
- Gunkel, M., Erdel, F., Rippe, K. *et al.* (2009) Dual color localization microscopy of cellular nanostructures. *Biotechnol. J.* **4**, 927–938.
- Heilemann, M., Herten, D.P., Heintzmann, R. *et al.* (2002) High-resolution colocalization of single dye molecules by fluorescence lifetime imaging microscopy. *Anal. Chem.* **74**, 3511–3517.
- Heilemann, M., van de Linde, S., Schuettelpelz, M. *et al.* (2008) Subdiffraction-resolution fluorescence imaging with conventional fluorescent probes. *Angew. Chem. Int. Ed.* **47**, 6172–6176.
- Hendrix, J., Flors, C., Dedecker, P., Hofkens, J. & Engelborghs, Y. (2008) Dark states in monomeric red fluorescent proteins studied by fluorescence correlation and single molecule spectroscopy. *Biophys. J.* **94**, 4103–4113.
- Hess, S.T., Girirajan, T.P.K. & Mason, M.D. (2006) Ultra-high resolution imaging by uorescence photoactivation localization microscopy. *Biophys. J.* **91**, 4258–4272.
- Hildenbrand, G., Rapp, A., Spoeri, U., Wagner, C., Cremer, C. & Hausmann, M. (2005) Nano-sizing of specific gene domains in intact human cell nuclei by spatially modulated illumination light microscopy. *Biophys. J.* **88**, 4312–4318.
- Kaufmann, R., Lemmer, P., Gunkel, M. *et al.* (2009) SPDM – Single molecule superresolution of cellular nanostructures. *Proc. SPIE* **7185**, 1–19.
- King, C.R., Kraus, M.H. & Aaronson, S.A. (1985) Amplification of a novel v-erbB-related gene in a human mammary carcinoma. *Science* **229**, 974–976.
- Lemmer, P., Gunkel, M., Baddeley, D. *et al.* (2008) SPDM: light microscopy with single-molecule resolution at the nanoscale. *Appl. Phys. B* **93**, 1–12.
- Lemmer, P., Gunkel, M., Baddeley, D. *et al.* (2009) Using conventional fluorescent markers for far-field fluorescence localization nanoscopy allows resolution in the 10 nm regime. *J. Microsc.* **235**, 163–171.
- Nagy, P., Jenei, A., Kirsch, A.K., Szollosi, J., Damjanovich, S. & Jovin, T.M. (1999) Activation-dependent clustering of the erbB2 receptor tyrosine kinase detected by scanning near-field optical microscopy. *J. Cell Sci.* **112**, 1733–1741.
- Pachmann, K., Heiß, P., Demel, U. & Titz, G. (2001) Detection and enumeration of minimal numbers of circulating tumour cells in peripheral blood using laser scanning cytometry. *Clin. Chem. Lab. Med.* **39**, 811–817.
- Pachmann, K., Camara, O., Kavallaris, A., Schneider, U., Schünemann, S. & Höffken, K. (2005a) Quantification of the response of circulating epithelial cells to neoadjuvant treatment for breast cancer: a new tool for therapy monitoring. *Breast Cancer Res.* **7**, 975–979.
- Pachmann, K., Clement, J.H., Schneider, C.P., Willen, B., Camara, O., Pachmann, U. & Höffken, K. (2005b) Standardized quantification of circulating peripheral tumor cells from lung and breast cancer. *Clin. Chem. Lab. Med.* **43**, 617–627.
- Patterson, G.H. & Lippincott-Schwartz, J. (2002) A photoactivatable GFP for selective photolabeling of proteins and cells. *Science* **297**, 1873–1877.
- Popescu, N.C., King, C.R. & Kraus, M.H. (1989) Localization of the human erbB-2 gene on normal and rearranged chromosomes 17 to bands q12–21.32. *Genomics* **4**, 362–366.
- Rayleigh, L. (1896) On the theory of optical images, with special reference to the microscope. *Philos. Mag.* **42**, 167–195.
- Reymann, J., Baddeley, D., Gunkel, M. *et al.* (2008) High-precision structural analysis of subnuclear complexes in fixed and live cells via spatially modulated illumination (SMI) microscopy. *Chromosome Res.* **16**, 367–382.
- Ring, A., Smith, I. E. & Dowsett M. (2004) Circulating tumour cells in breast cancer. *The Lancet Oncology* **5**, 79–88.
- Rust, M.J., Bates, M. & Zhuang, X. (2006) Sub-diffraction-limit imaging by stochastic optical reconstruction microscopy (STORM). *Nat. Methods* **3**, 793–795.
- Schechter, A.L., Stern, D.F., Vaidyanathan, L., Decker, S.J., Drebin, J. A., Greene, M.I. & Weinberg, R.A. (1984) The neu oncogene: an erbB-related gene encoding a 185,000-Mr tumour antigen. *Nature* **312**, 513–516.
- Sieber, J.J., Willig, K.I., Kutzner, C. *et al.* (2007) Anatomy and dynamics of a supramolecular membrane protein cluster. *Science* **317**, 1072–1076.
- Sinnecker, D., Voigt, P., Hellwig, N. & Schaefer, M. (2005) Reversible photobleaching of enhanced green fluorescent proteins. *Biochemistry* **44**, 7085–7094.
- Slamon, D.J., Clark, G.M., Wong, S.G., Levin, W.J., Ullrich, A. & McGuire, W.L. (1987) Human breast cancer: correlation of relapse and survival with amplification of the HER-2/neu oncogene. *Science* **235**, 177–182.
- Slamon, D.J., Godolphin, W., Jones, L.A. *et al.* (1989) Studies of the HER-2/neu proto-oncogene in human breast and ovarian cancer. *Science* **244**, 707–712.
- Stern, D.F., Heffernan, P.A. & Weinberg, R.A. (1986) p185, a product of the neu proto-oncogene, is a receptor-like protein associated with tyrosine kinase activity. *Mol. Cell. Biol.* **6**, 1729–1740.
- Warren, C.M. & Landgraf, R. (2006) Signaling through ERBB receptors: multiple layers of diversity and control. *Cell Signal* **18**, 923–933.
- Yang, S., Raymond-Stintz, M.A., Ying, W. *et al.* (2007) Mapping ErbB receptors on breast cancer cell membranes during signal transduction. *J. Cell Sci.* **120**, 2763–2773.
- Yarden Y. & Sliwkowski M.X. (2001) Untangling the ErbB signalling network. *Nat. Rev. Mol. Cell. Biol.* **2**, 127–137.